ARL-TR-9197 • MAY 2021

DEVCOM ARMY RESEARCH LABORATORY

Demonstration of a Radioisotope Power Source Using Promethium-147 Chloride and 4H-SiC Betavoltaic Cell

by Marc Litz, Johnny Russo, and Brenda Smith

NOTICES

Disclaimers

The findings in this report are not to be construed as an official Department of the Army position unless so designated by other authorized documents.

Citation of manufacturer's or trade names does not constitute an official endorsement or approval of the use thereof.

Destroy this report when it is no longer needed. Do not return it to the originator.

ARL-TR-9197 ● MAY 2021

Demonstration of a Radioisotope Power Source Using Promethium-147 Chloride and 4H-SiC Betavoltaic Cell

Marc Litz
Sensors and Electron Devices Directorate, DEVCOM Army Research Laboratory

Johnny Russo
University of Maryland

Brenda Smith
Oak Ridge National Lab

REPORT DOCUMENTATION PAGE

Form Approved
OMB No. 0704-0188

1. REPORT DATE *(DD-MM-YYYY)*	2. REPORT TYPE	3. DATES COVERED (From - To)
May 2021	Technical Report	1 April 2020–1 March 2021

4. TITLE AND SUBTITLE
Demonstration of a Radioisotope Power Source Using Promethium-147 Chloride and 4H-SiC Betavoltaic Cell

5a. CONTRACT NUMBER

5b. GRANT NUMBER

5c. PROGRAM ELEMENT NUMBER

6. AUTHOR(S)
Marc Litz, Johnny Russo, and Brenda Smith

5d. PROJECT NUMBER

5e. TASK NUMBER

5f. WORK UNIT NUMBER

7. PERFORMING ORGANIZATION NAME(S) AND ADDRESS(ES)
DEVCOM Army Research Laboratory
ATTN: FCDD-RLS-CC
Adelphi, MD 20783-1138

8. PERFORMING ORGANIZATION REPORT NUMBER
ARL-TR-9197

9. SPONSORING/MONITORING AGENCY NAME(S) AND ADDRESS(ES)
NASA

10. SPONSOR/MONITOR'S ACRONYM(S)

11. SPONSOR/MONITOR'S REPORT NUMBER(S)

12. DISTRIBUTION/AVAILABILITY STATEMENT
Approved for public release: distribution unlimited.

13. SUPPLEMENTARY NOTES
ORCID ID: Marc Litz, 0000-0003-0694-4152

14. ABSTRACT

Unattended, compact terrestrial and space sensors require power sources that have high energy and power density to continuously operate for 3 to 25 years depending on application. Currently, chemical sources cannot fully satisfy these conditions. Radioisotope power sources using β^--emitting radioisotopes have energy densities 1000× greater than chemical sources. Their power density is a function of β- flux saturation in the planar (2-D) configuration, β^- emission range in the semiconductor converter, and betavoltaic (βV) or beta-photovoltaic (β-PV) cell geometry. Using state-of-the-art (SOA) 4H-SiC βV cell and 2-D configuration, promethium-147 (^{147}Pm) is the only β^--emitting radioisotope that can match power density with chemical sources while surpassing them in energy density. This approach to match power density while sustaining the unmatchable energy density is described. Promethium-147(III) chloride ($^{147}PmCl_3$) and 4H-SiC βV cell were used for the 2-D configuration nuclear power source. The $^{147}PmCl_3$ dried layers were sensitive to laboratory air moisture. The dried layers absorbed the external moisture and lowered the maximum power point (MPP) of the βV cell. Moisture controllability through continuous heating during dispensing and placement in airtight enclosures during I-V curve measurements lessened the moisture absorption negative effects shown by increasing MPP. A total activity of 1,680 mCi/cm^2 was deposited on a 4H-SiC βV cell. A MPP of ≈3.2 μW/cm^2 was generated after source drying period. MPP saturation point was not reached at 1,680 mCi/cm^2. This extrapolates to ≈6.4 μW/cm^2 of $^{147}PmCl_3$ in between 2× 4H-SiC making a battery packet and ≈64 μW/cm^3 with 10× packets at 1 cm^2. At this power density, the nuclear power source could supply milliwatts to various sensors for at least 3 years continuously in a 1000 cm^3 total volume.

15. SUBJECT TERMS
Place Betavoltaic, $^{147}PmCl_3$, 4H-SiC

16. SECURITY CLASSIFICATION OF:			17. LIMITATION OF ABSTRACT	18. NUMBER OF PAGES	19a. NAME OF RESPONSIBLE PERSON
a. REPORT	b. ABSTRACT	c. THIS PAGE			Marc Litz
Unclassified	Unclassified	Unclassified	UU	17	19b. TELEPHONE NUMBER (Include area code) (301) 394-5556

Contents

List of Figures

Acknowledgments

The 4H-SiC described in this report was designed, grown, and prepared for packaging by Chris Thomas, Widetronix Inc., under an SBIR agreement.

1. Introduction

Unattended terrestrial and orbital (exosphere and outer-space) sensors are of growing interest for private, government, and military operations. Sensor multi- and singular capabilities, operation time, and synergy superiority are important for job outcome. The volume size of these remote sensors has reduced while capabilities have increased due to mission requirements. A high-energy and power-dense source is essential to satisfy the sensor capability increase. Most importantly, the power source's volume should be a small percentage of the total volume of the sensor. Current chemical power sources cannot satisfy these remote sensor requirements of constant milliwatt power for multiple years while retaining a minimum volume specification. Beta (β^-) and alpha (α) emitting radioisotopes have the potential to satisfy these requirements. The Alternative Energy Team at the US Army Combat Capabilities Development Command Army Research Laboratory is currently investigating four commercially available radioisotopes: tritium (^{3}H), nickel-63 (^{63}Ni), promethium-147 (^{147}Pm), and americium-241 (^{241}Am). Energy densities of all four radioisotopes are more than 1000× greater than chemical sources.[1]

In this report, an approach to surpass current nuclear battery power performances was established through the improvement of the source efficiency (η_β) while attempting to increase surface power density (P_{nuc}) using promethium-147(III) chloride ($^{147}PmCl_3$) in solution form. The nuclear power source followed a direct conversion system where the radioisotope/fuel source is the $^{147}PmCl_3$ and the semiconductor converter is a planar 4H-SiC betavoltaic (βV) cell. Two nuclear power sources were assembled and tested. The $^{147}PmCl_3$ solution was dispensed on two 4H-SiC βV cells inside a 700-µm tall, borosilicate reservoir. Current and voltage (I-V) curves were recorded after solvent evaporated and radioisotope solution dried down to a coating layer. Moisture controllability was performed on only one nuclear power source to identify negative moisture effects. Electrical power and total conversion efficiency (η_t) of both nuclear power sources were measured, calculated, and compared.

2. Experimental Preparation and Test

All nuclear power sources' assembly and testing were performed at Oak Ridge National Laboratory (ORNL) inside of a fume hood. Two 4H-SiC βV cells from Widetronix Inc. were used as the semiconductor converters.[2] All βV cells were placed in a light-tight and airtight enclosure, providing a completely dark and low-moisture environment. A bottomless, borosilicate reservoir with an inner diameter

of 3 mm, frame outer diameter of 4.3 mm, area of 0.0706 cm^2, and thickness of 700 µm was adhered to the 4H-SiC surface using a UV curable epoxy (Fig. 1).

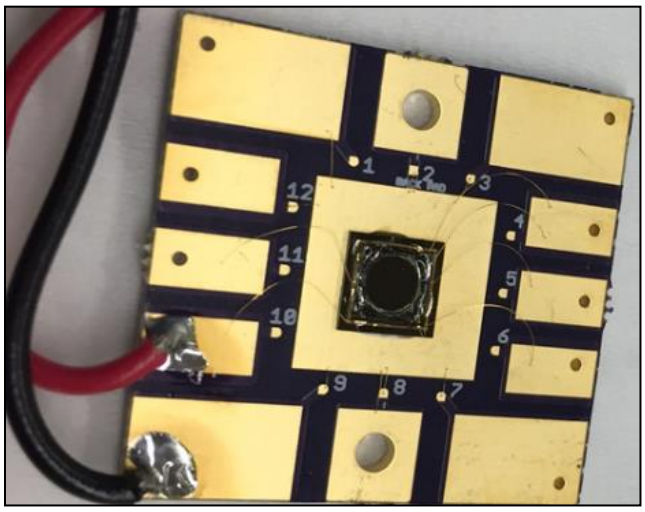

Fig. 1 A 4H-SIC converter is mounted on a conducting pad with conductive epoxy. The electrodes are wire bonded to pads on the mounting board for easy access during experimental measurement of I-V curves.

The βV cell's I-V curve and leakage current were measured by a Keithley 2450 SourceMeter using four-terminal sensing (Kelvin sensing, 4 Wire). An I-V curve trace was continuously measured for 5 min until there were no changes in the measurement demonstrating stable ambient environmental conditions. After this step, a final I-V curve trace was measured from the sourcemeter. The maximum power point (MPP) was calculated from the I-V curve, representing the electrical power output. The βV cell was measured at standard ambient temperature and pressure (SATP) in a fume hood.

The $^{147}PmCl_3$ was purchased from Eckert & Ziegler Analytics Inc. and handled by the US Department of Energy Office of Science by the Isotope Program in the Office of Nuclear Physics. The $^{147}PmCl_3$ was stored in a 10-mL ampoule with 0.5 mol/l HCl solution. Prior to use, the $^{147}PmCl_3$ was washed with distilled water and dried three times and finally re-suspended in a 1:5 vol ratio of toluene to ethanol at a concentration of 1.30 mCi/µL. This procedure removed the HCl, leaving just the $^{147}PmCl_3$ and 1:5 vol ratio of toluene and ethanol. The radioactivity concentration was 1.19 mCi/µL at experiment starting date. A micropipette was used to dispense the radioisotope onto the βV cells inside the reservoir. The radioisotope solution was evaporated down using a heat plate at a temperature range from 125 °C to 150 °C. Three camera microscopes at different orientations recorded the evaporation of the solvent and imaged the $^{147}PmCl_3$ coatings (Fig. 2a). After dispensing and heating, the nuclear power sources were placed in airtight

enclosures filled with Drierite and silica gel for moisture controllability during each I-V curve measurement. After radioisotope dispensing and I-V curve measurements, the two devices were connected to a Keithley 6485 Picoammeter for long-term current measurements to observe potential MPP reduction caused by βV cell degradation from high-energy β^--emitting particles and moisture absorption (Fig. 2).

(a) (b)

Fig. 2 a) Multiple magnifying microscopes were mounted in fume hood in order to measure flow of isotope on energy converter and final thickness of isotope deposition. b) In order to measure degradation in isotope or energy conversion materials, an automated data acquisition system was configured adjacent to the fume hood to measure the output current of the fabricated isotope devices.

On Day 1 of testing, droplets of 2 µL were dispensed on the first 4H-SiC βV cell, Device 34, for each I-V curve measurement. For Device 34, heating was not applied during droplet dispensing while images and videos were taken before and after each I-V curve measurement for the first 28 µL. Heating for 2 min at 150 °C was applied after MPP started reducing at a total volume of 28 µL (33.32 mCi at 1.19 mCi/µL). MPP slightly increased after heating was performed. This was the last measurement for day 1. The power source was placed in the same light-tight and airtight enclosure with Drierite and silica gel overnight.

On day 2 of testing, Device 34 was measured again, and the MPP decreased from 1.35 µW/cm^2 to 0.90 µW/cm^2. Microscope images were taken of the power source surface. A large gap was seen on the surface (Fig. 3a). The power source was then placed on the heat plate for 2.5 min at 140 °C. Microscope images show a more uniform surface and the large gap in the center was not noticeable (Fig. 3b). Additional I-V curve measurements were made after the first heating. After the second I-V curve measurement, the MPP slightly decreased from 0.968 µW/cm^2 to 0.966 µW/cm^2. Another microscope image showed the uniform surface slightly

changed after the initial heating when placed outside of the enclosure. Three I-V curve measurements were recorded for a total dispensed volume of 34, 40, and 46 µL. Heating was applied after dispensing for 4 min at 140 °C for each total dispensed volume. The MPP as a function of dispensed radioactivity started to saturate after 571 mCi/cm^2 (34 µL) with a MPP of 1.27 µW/cm^2. The total conversion efficiency (η_t) at a dispensed activity 571 mCi/cm^2 was 1.21% based on an average β^- energy of 61.93 keV. After the last measurement was recorded, the power source was placed in the light-tight and airtight enclosure with Drierite and silica gel.

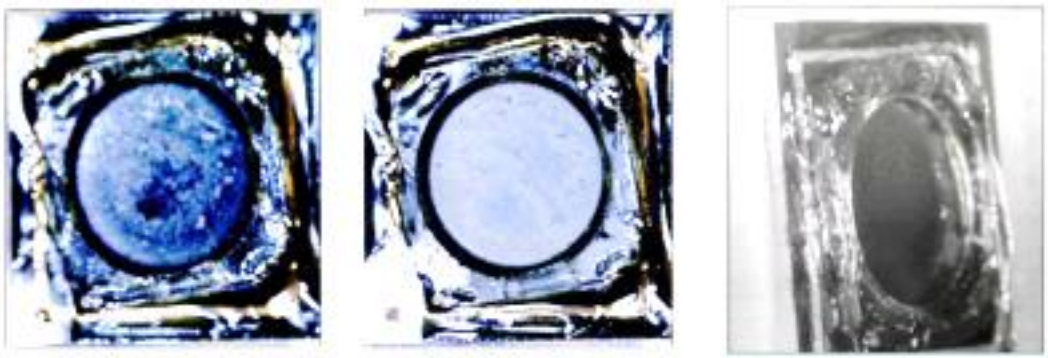

(a) (b) (c)

Fig. 3 147PMCL3 was dispensed within a 3-mm diameter, 700-µm tall reservoir ON4H-sicenergy converter. Isotope was dropped from micropipette into reservoir, where evaporation of toluene and ethylene left the residue of 147PMCL3. a) The liquid format radioisotope did not dry uniformly within the reservoir with less than 10 µL applied. b) After application of 25 µL of liquid format isotope, the layer became uniform. c) Offset view.

The second set of measurements on day 2 were performed on Device 26. Droplets of 2 µL were dispensed into reservoir. I-V curve measurements were recorded after dispensing 10 µL of total volume. Also, heating was applied at 125 °C for 2 min after dispensing a total volume of 10 µL. This process was repeated six times, reaching a total volume of 60 µL on day 2. Only microscope images at 20 µL and 30 µL were taken. After the last measurement was recorded, the power source was placed in the light-tight and airtight enclosure with Drierite and silica gel. On day 3 of testing, Device 26 was measured again, and the MPP increased from 1.97 to 2.17 µW/cm^2. The day 2 process was repeated four times, reaching a total volume of 100 µL on day 3. Microscope images were taken after the last 10 µL were dispensed and heated. The MPP was 3.19 µW/cm^2 at a total radioactivity of 119 mCi (1,680 mCi/cm^2) and η_t of 1.04%. A quadratic curve-fit forecasts that saturation point can be potentially reached at 2500 mCi/cm^2 with a MPP of 3.65 µW/cm^2.

Devices 26 and 34 showed different electrical properties as the radioactivity increased even though their leakage currents were very similar before radioisotope

dispensing occurred. For Device 26, the MPP saturation point could not be reached, whereas Device 34's MPP saturation point was reached at a radioactivity of 571 mCi/cm^2. Device 34 had higher electrical properties from 33.6 to 470 mCi/cm^2. Device 26 had constant FF and η_t of 59.8 ± 4.72% and 1.169 ± 0.166%, respectively, as a function of increasing radioactivity. The major difference between each power source was the dispensing process. Device 34 was exposed to the laboratory air for a longer period. More surface images were taken compared to the Device 26 process, and solvent evaporation videos were recorded, whereas no videos were recorded for Device 26. Also, 15 I-V curve measurements were taken compared to 11× I-V curve measurements for Device 26. Approximately 6 µL was dispensed compared to 10 µL for Device 26 before most of the I-V curve measurements. Figures 4a and b show the MPP and η_t as a function of dispensed radioactivity. Most importantly, heating was not performed until after 28 µL dispensed on Device 34 solvent were completely evaporated at SATP.

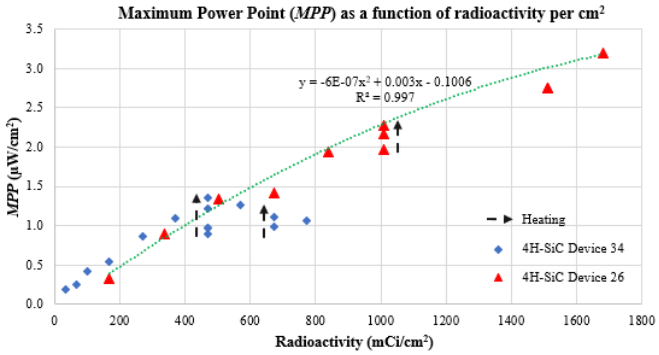

(a)

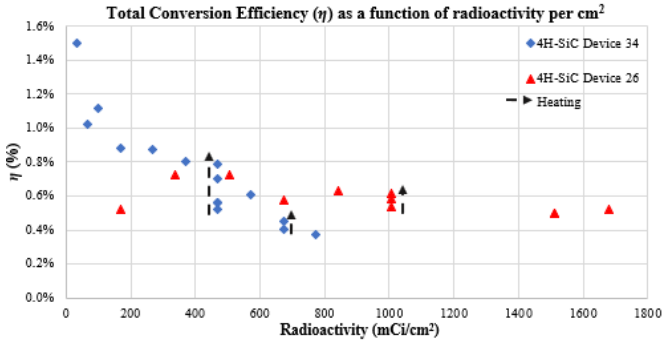

(b)

Fig. 4 147PMCL3: a) MPP, b) efficiency (η) as a function of dispensed radioactivity for both 4H-SIC devices

Microscope images show visible evidence of surface effects from prolonged exposure to laboratory air moisture inside of a fume hood. The visible evidence is prominent in microscope images of Device 34, specifically at a total activity of 28 µL (Figs. 5a to d). Device 34 was heated between each I-V curve measurement

and microscope image. The surface changes from rough, having several unique features and gaps, and wet to uniform and dry because of the heating. In addition, the MPP would increase after each heating process. It was quite evident that the $^{147}PmCl_3$ coating was sensitive to air moisture once the solvent evaporated. The MPP would decrease because of the moisture absorption on the surface, which mostly occurred during the microscope camera focusing and imaging procedure. Device 26 had a higher MPP, mostly due to exposure to the laboratory air moisture being minimized and constant heating. Also, coating formations were different for each device. This difference was apparent when comparing microscope images of Devices 34 and 26 (Figs. 5e and f). For Device 34, the coating was more uniform except for the concentric ring around the perimeter of the reservoir inner diameter. Device 26 had two concentric rings: one at the perimeter of the reservoir inner diameter and another offset to the center. As more and more radioactivity was dispensed, these concentric rings became less prominent on both devices. Nevertheless, Device 34 reached its MPP saturation far sooner than Device 26 because heating was not immediately applied after 28 μL, which could have trapped a significant volume of water vapor causing significant β^- energy absorption, and the prolonged exposure to air moisture due to the microscope imaging procedure.

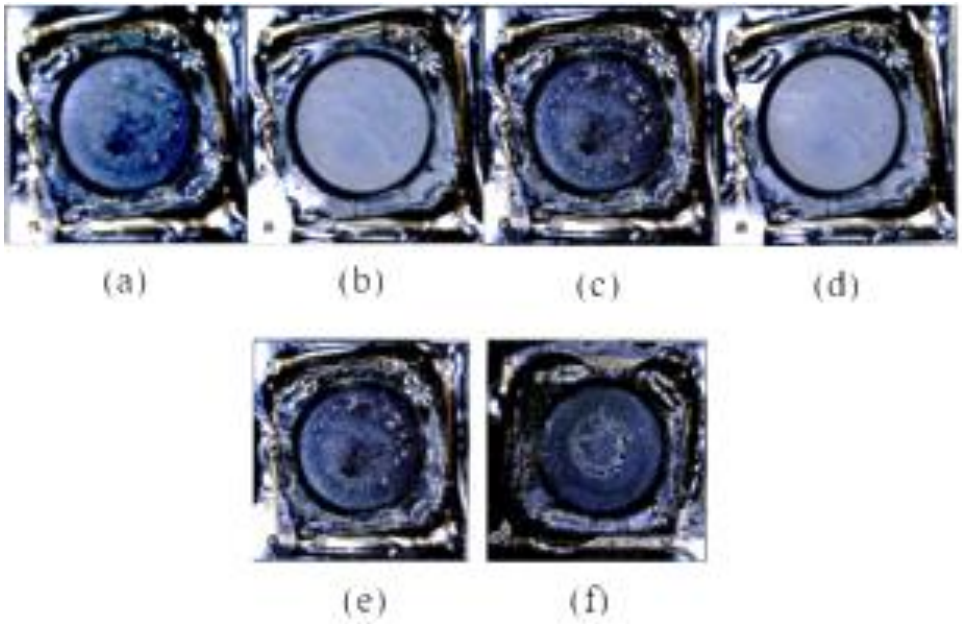

Fig. 5 Images of Device 34: a) to d) with dried 147PMCL3; images of Device 26: e) and f) with dried 147PMCL3

3. Conclusion

In summary, nuclear power sources using a planar 4H-SiC βV cells and $^{147}PmCl_3$ were designed, constructed, and tested. For Device 26, MPP constantly increased while the FF and ηt stayed constant as radioactivity increased. Device 34's electrical properties were initially higher than Device 26 from 33.6 to 470 mCi/cm^2. However, as the dispensed total activity increased higher than 571 mCi/cm^2, a temporary saturation point was reached. The follow-on test results show that absorbed moisture was the culprit, and moisture control is pivotal when using $^{147}PmCl_3$ as the radioisotope source. When applying heat and lessening the moisture exposure, the MPP started increasing at the same dispensing radioactivity. When the moisture was not minimized or lowered from the experiment, the MPP would decrease and reach a saturation point even after more radioactivity was added on, which was shown with test results from Devices 34 and 26. For Device 26, a MPP of ≈3.2 μW/cm^2 was generated at a total activity of 1,680 mCi/cm^2, FF of 65.3%, and ηt of 1.12%. This extrapolates to ≈6.4 per 1 cm^2 of $^{147}PmCl_3$ in between 2× 4H-SiC making a battery packet and ≈64 μW/cm^3 with 10× packets at 1 cm^2. At this power density, the nuclear power source could supply milliwatts to various sensors for at least 3 years continuously in a 1000-cm^3 total volume. Furthermore, MPP saturation point was not reached at 1,680 mCi/cm^2. A quadratic curve-fit forecasts the highest MPP to be 3.65 μW/cm^2 at a total radioactivity of 2500 mCi/cm^2. Potential areas of higher MPP are through complete moisture controllability using a glove box, increasing specific activity using different ^{147}Pm liquid or slurry form, and increasing 4H-SiC aspect ratio from planar to etched or grown microstructures.

4. References

1. Romer M, Miley GH, Luo N, Gimlin RJ. Ragone plot comparison of radioisotope cells and the direct sodium borohydride/hydrogen peroxide fuel cell with chemical batteries. IEEE T Energy Conver. 2008;23(1):171–178.
2. Thomas C, Portnoff S, Spencer MG. High efficiency 4H-SiC betavoltaic power sources using tritium radioisotope. Appl Phys Lett. 2016;108(1):013505.

List of Symbols, Abbreviations, and Acronyms

^{3}H	tritium
^{63}Ni	nickel-63
^{147}Pm	promethium-147
$^{147}PmCl_3$	promethium-147(III) chloride
^{241}Am	americium-241
α	alpha
β^-	beta
βV	betavoltaic
I-V	current and voltage
MPP	maximum power point
ORNL	Oak Ridge National Laboratory
SATP	standard ambient temperature and pressure
SOA	state-of-the-art
UV	ultraviolet

1 (PDF)	DEFENSE TECHNICAL INFORMATION CTR DTIC OCA
1 (PDF)	DEVCOM ARL FCDD RLD DCI TECH LIB
1 (PDF)	DEVCOM ARL FCDD RLS CC M LITZ
1 (PDF)	UNIVERSITY OF MARYLAND J RUSSO
1 (PDF)	OAK RIDGE NATIONAL LAB B SMITH